Stanford Exploration Project, Report 97, July 8, 1998, pages 61–72

Stanford Exploration Project, Report 97, July 8, 1998, pages 61–72

Accurate linear interpolation in the extended split-step migration

Hermes Malcotti and Biondo Biondi[1]

keywords: *migration, split-step, extended*

ABSTRACT

We present an implementation of the extended split-step migration method for strong lateral velocity gradients. Steep events are imaged by using the evanescent energy in the linear interpolation of different downward continued wavefields in every depth step and between reference velocities. The 3-D algorithm is a 3-D prestack operator based on common-azimuth continuation at every depth step. We show the extended split-step impulse response with a strong lateral velocity gradient of 0.5 s^{-1}, and we apply the migration algorithm over two synthetic data sets: a 2-D salt dome model and the 3-D SEG-EAEG data set. In addition, we show the resulting prestack migrated image of the real data set that used to built the 2-D salt dome model. Our results show that the evanescent energy is important in the linear interpolation to preserve steep events in a strong lateral velocity gradient.

INTRODUCTION

The split-step method is a mixed domain operator (ω-x) that adapts a lateral velocity variation. Different approximations for split-step migration have been published ((Herbert, 1992; Kessinger, 1992; Biondi and Palacharla, 1996; Huang and Fechler, 1997)). Stoffa et al. (1990) introduced the split-step method to migrate post-stack data using one reference velocity. In contrast, the extended split-step algorithm uses more than one reference velocity to accommodate lateral velocity variations, similar to the way that phase-shift-plus-interpolation works (Gazdag and Sguazzero, 1984).

The split-step algorithm solves the wave equation in ω-space coordinates. The downward continuation of a wavefield using a split-step algorithm has two parts: the wavefield is first downward continued with a phase shift defined by the DSR operator with a constant reference velocity (equation 2, or focusing term); this is then followed by a vertical time shift correction in the space domain applied to the continued wavefield proportional to the contrast in slowness.

[1] **email:** hermes@sep.stanford.edu, binodo@sep.stanford.edu

In a strong lateral velocity gradient, the split-step migration does not properly image steep reflectors when k_z wavenumbers are limited to avoid evanescent energy (i.e., solving the one-way wave equation). Two consecutive reference velocities define the interval where the required downward continued wavefield for the mapping velocity needs to be interpolated. In general, these wavefields are downward continued by applying a phase shift defined by the vertical depth-wavenumber, k_z, as a real function of the migration dips. This last assumption limits the interpolation of the continued wavefields for a velocity between two reference velocities because dips at low velocities correspond to dips at higher reference velocity, and those dips could be lying in the evanescent region of the higher reference velocity (Kessinger, 1992).

In this paper, we show that including the evanescent energy in the k_z-domain helps to obtain an accurate interpolated downward continued wavefield for every migration depth step. Three different data sets are used to make comparisons between extended split-step migration with and without evanescent energy.

In addition, we have an economical 3-D extended split-step prestack migration based on the common-azimuth downward continuation of the wavefield. Common-azimuth migration is based on the stationary-phase approximation of the 3-D DSR in every downward continuation of the wavefield, resulting in a DSR operator independent of the in-line-offset wavenumber (Biondi and Palacharla, 1996).

EXTENDED SPLIT-STEP USING EVANESCENT ENERGY

For the downward continuation of the wavefield, the DSR in the $\omega - k$ domain is chosen to be always real to avoid the seismic evanescent energy. In the $\omega - k$ space the DSR operator is the following:

$$\begin{aligned} & DSR(k_m, k_h, z, \omega) = \\ & \sqrt{\frac{\omega^2}{v^2_{(mS,z)}} - \frac{1}{4}((k_{mx} - k_{hx})^2 + (k_{my} - k_{hy})^2)} \\ + \; & \sqrt{\frac{\omega^2}{v^2_{(mG,z)}} - \frac{1}{4}((k_{mx} + k_{hx})^2 + (k_{my} + k_{hy})^2)} \end{aligned} \tag{1}$$

Applying the split-step approximation to the DSR operator, we obtain

$$\begin{aligned} & DSR(k_m, k_h, z, \omega) \cong \\ & \sqrt{\frac{\omega^2}{v^2_{Sref,z}} - \frac{1}{4}((k_{mx} - k_{hx})^2 + (k_{my} - \overline{k}_{hy})^2)} \\ + \; & (\frac{\omega}{v_{mS,z}} - \frac{\omega}{v_{Sref}, z}) \\ + \; & \sqrt{\frac{\omega^2}{v^2_{(Gref,z)}} - \frac{1}{4}((k_{mx} + k_{hx})^2 + (k_{my} + \overline{k}_{hy})^2)} \end{aligned}$$

$$+ \quad (\frac{\omega}{v_{(mG,z)}} - \frac{\omega}{v_{Gref,z}}), \tag{2}$$

where k_{mx} is the CDP in-line wavenumber, k_{my} is the CDP cross-line wavenumber, k_{hx} is the offset in-line wavenumber and $\overline{k}_{hy}$ is the offset cross-line wavenumber, $v_{mG,z}$ and $v_{mS,z}$ are the velocity fields for source and geophone midpoint-coordinates and $v_{Sref,z}$ and $v_{Gref,z}$ are the set of the reference velocities for every depth.

The vertical wavenumber k_z in a conventional downward continuation is a real number (equation 2) avoiding the evanescent energy. Therefore, in the 2-D prestack case, k_z is calculated by setting $\frac{\omega^2}{v^2} > \frac{1}{4}(k_{mx} \pm k_{hx})^2$. This condition guarantees that k_z is real, and it rejects the energy that corresponds to imaginary k_z or the evanescent energy domain. In the case of an extended split-step migration, the evanescent energy is useful for interpolating two downward continued wavefields.

Figure 1 shows the values of k_z for 10 different reference velocities associated with receiver locations for the zeror-offset case. The outer curve corresponds to a low reference velocity (1500m/s) and the inner curve corresponds to a high velocity (5000m/s). The phase correction to downward continue the wavefield in one depth step is the positive vertical wavenumbers k_z multiplied by the depth step. The negatives k_z multiplied by a depth step represent the argument of a damped exponential applied to the wavefield that is traveling with an angle sine greater than one. Figure 1 also shows that dips at a higher reference velocity correspond to smaller dips at a lower reference velocity, when k_z is linear interpolated between two different reference velocities.

In addition, Figure 1 helps to define the evanescent energy nesccesary to image steep events. The k_z values for the minimun velocity define the the evanescent energy necessary for imaging steep events for a depth z. Setting this new limit for the k_z helps to save computer time.

In order to preserve very steep dips during the linear interpolation between two downward continued wavefields, the k_z domain must be extended (Fig. 1). Therefore, in our extended split-step algorithm, instead of rejecting imaginary values of the 2-D DSR, we save and use those values in the interpolation of downward continued wavefields. Gazdag (1984) presented a different approach, where evanescent energy is used in a phase-shift-plus-interpolation migration by replacing the imaginary values of k_z for values calculated using a straight line tangent to a k_z curve from a specific angle.

The 3-D prestack downward continuation operator in common-azimuth is based on a stationary-phase approximation of the 3-D DSR (equation 1). This approximation reduces the dimensionality of the downward continuation operator from 5 to 4 dimensions, constraining the direction of propagation of source and receiver rays to the same plane and azimuth, and calculating the cross-line-offset wavenumbers ($\overline{k}_{hy}$) from the in-line (k_{mx}) and cross-line CDP wavenumbers (k_{my}) and in-line offset wavenumbers (k_{hx}) (Biondi and Palacharla, 1996).

RESULTS

The implementation of the extended split-step migration for 2-D and 3-D prestack data sets have been tested on different synthetic models. Figure 2 we show the 2-D impulse response of the migration operator for zero-offset migration, using a velocity field with a strong lateral and vertical gradient equal to $0.5s^{-1}$ (the direction of the gradient is in the same direction that the coordinate increases).

Figure 2 shows the impulse responses using 10 reference velocities for the zero-offset case. Figure 2 (left) plots the impulse response of the extended split-step migration with a real vertical wavenumber. This impulse response shows that the migration is dip limited.

The impulse response in Figure 2 (right) shows how the evanescent energy helps to increase the maximum dip handled by the split-step migration. Moreover, the evanescent energy is more important in the low velocity areas of the velocity model (small in-line coordinates).

When evanescent energy is used during the interpolation of the downward continued wavefields with different reference velocities, the extended split-step migration can handle steeper events. Therefore, extending both the range in the vertical wavenumber domain, kz, and the number of reference velocities improves the image obtained with the extended split-step migration in areas with a strong velocity lateral gradient.

Figure 10 shows a geological model in the North Sea used in a 2-D finite-difference modeling provided by ELF and CCG. This geological model represents the rise of a salt diapir, characterized by a strong lateral velocity gradient in the seismic cable length. The seismic synthetic data set has the following acquisition parameters: source spacing 50m; receiver spacing 25m; final CMP spacing 12.5m; near-offset 170m; far-offset 3350m; maximum recorded time 5s; and time sampling 4ms.

Figure 6 shows the extended split-step prestack migration with evanescent energy using 5 reference velocities and a maximum offset 800m. Using fewer offsets it was possible to image the very steep event located below the shallow salt body. Comparing this image with the prestack image using all the offsets (Fig. 6), the amplitude of the steep events is very low relative to the amplitude of the other reflectors, and this event disappears in the final zero-offset depth migrated section.

The other important imaging targets in this salt dome synthetic model are both the deeper flank of the salt dome (dipping at 43 deg) and the reflector just below the salt. In the prestack images (figs. 7 and 4), the bottom of the salt dome was not imaged using all the offsets. In contrast, this reflector was imaged in the prestack migration with a maximum offset of 800m because the energy of those reflectors exists on the near-offsets in migrated CDPs (Fig. 6 and 8). The coherent noise at the end of the depth section, should be attenuated by padding zeros at the end of the data set.

The real seismic data set of the mode in Figure (10) is a 3-D seismic survey.

I extracted the corresponding line to Figure (7) and applied a bandpass filter and stacked the traces of the two parallel lines in order to replace the missing or edited traces. Using a velocity field, different to the velocity in 10, we migrated it with the migration algorithm presented in this paper. The resulting prestack migrated image is plotted in Figure 9; it was migrated with 5 reference velocities. This migrated image shows that the modeling was used for just the important features of the geologic model (Figure 10). It is observed that the mean salt dome features that were discussed with the synthetic imaging results are imaged in the real data migrated image. For example, the steep event just below the small salt body is imaged, what it is missing is the base of the salt dome. We are working with the 3-D prestack data set of this real seismic data, in order to obtain a migrated image using the common-azimuth approximation.

The SEG-EAEG 3-D synthetic model was the third synthetic data set used to verify that our 3-D extended split step migration was correctly implemented. Figure 13 shows a cross-line section of the velocity data cube. This synthetic data set is characterized by a salt dome embedded in a linear vertical gradient, where salt and small salt features introduce a strong lateral gradient that affect the underlying horizontal reflectors.

Figures 12 and 14 show the 3-D extended split-step post-stack migration of the zero-offset cube SEG-EAEG model. The migration used 10 reference velocities to obtain this image. The bottom of the salt dome is well imaged below the salt irregularities in the top of the salt. Moreover, small lateral features and steep fault planes on the bottom of the salt dome are correctly imaged (see Fig. 13).

In order to improve this migration algorithm we are considering implementing a bilinear interpolation in the source and receiver axis of the downward continued wavefield. Using this bilinear interpolation we expect to reduce the number of reference velocities necessary to image steep reflectors in a velocity field with a lateral velocity gradient. In the case of diapirs, we want to hold the salt velocity constant for the downward continuation and use the linear interpolation of the wavefield elsewhere.

CONCLUSIONS

This work has presented a 2-D and 3-D extended split-step migration algorithm that uses the evanescent energy to image steep events in strong lateral gradients. Our results show that evanescent energy helps to image steep events in a strong lateral velocity gradients. In addition, the imaging of steep events depends on the number of reference velocities in order to accommodate the lateral velocity gradient, thus increasing the number of calculations.

ACKNOWLEDGMENTS

We thank Henri Calandra (ELF) and Patrice Ricarte (IFP) for the synthetic and real data set from the North Sea and interesting discussions. The first author thanks INTEVEP S.A. for financial support.

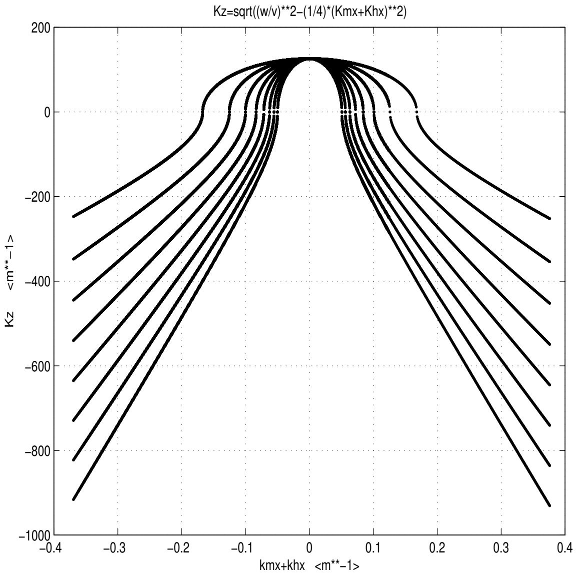

Figure 1: Receiver component of the dispersion equation of the extended split-step prestack migration for different reference velocities for the zero-offset case. Imaginary k_z are plotted as negative values. hermes1-kzdispesion [NR]

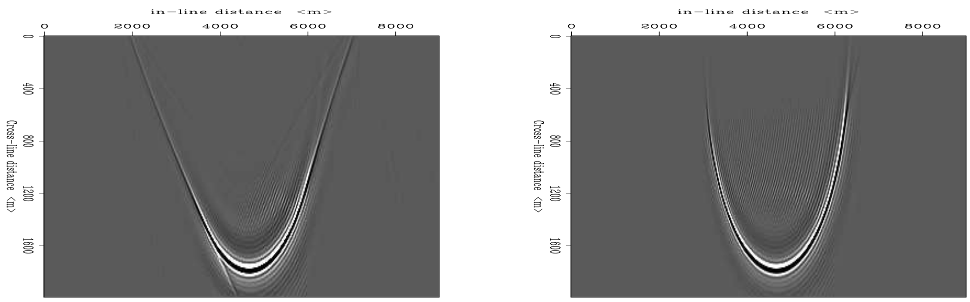

Figure 2: Impulse response with 10 reference velocities without (left) and with (right) evanescent energy in the linear interpolation. The velocity field has a lateral and vertical linear gradient of $0.5s^{-1}$. Notice that the migration operator using evanescent energy (figure on the right) can handle steeper events. hermes1-SPKEVANESZERO [CR]

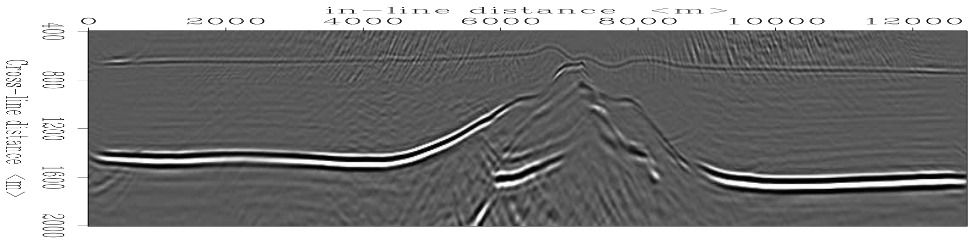

Figure 3: Extended split-step prestack migration without evanescent energy using 8 reference velocities. hermes1-ELFNOEVANESPRE2000 [CR]

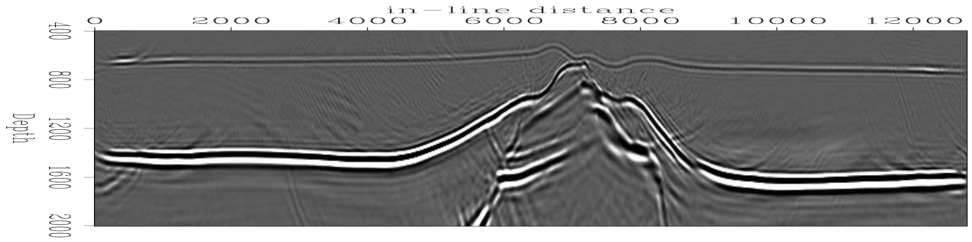

Figure 4: Extended split-step prestack migration using evanescent energy using 8 reference velocities (close up of Figure 8). hermes1-ELFEVANESPRE2000 [CR]

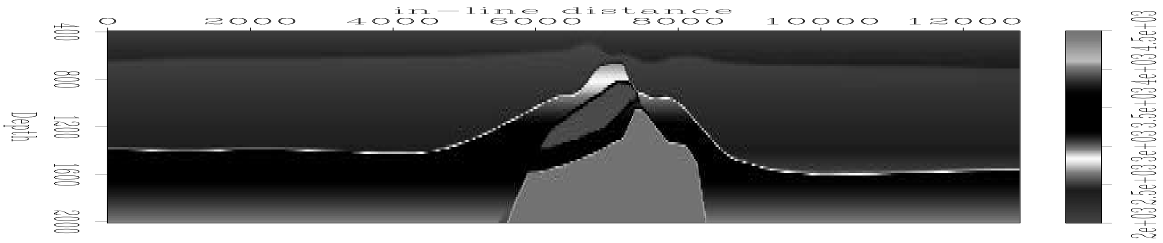

Figure 5: Close up of salt dome velocity model (ELF-IFP). hermes1-ELFVEL200 [CR]

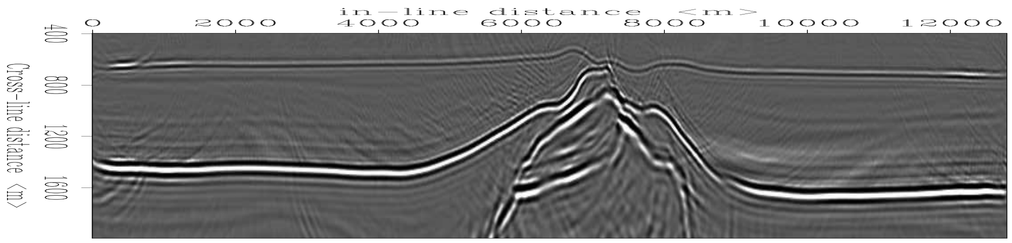

Figure 6: Extended split-step prestack migration with evanescent energy using 5 reference velocities and maximum offset 800m (Close up of Figure 8). Observe how the very steep events are imaged using fewer offsets. hermes1-ELFEVANESPRE32 [CR]

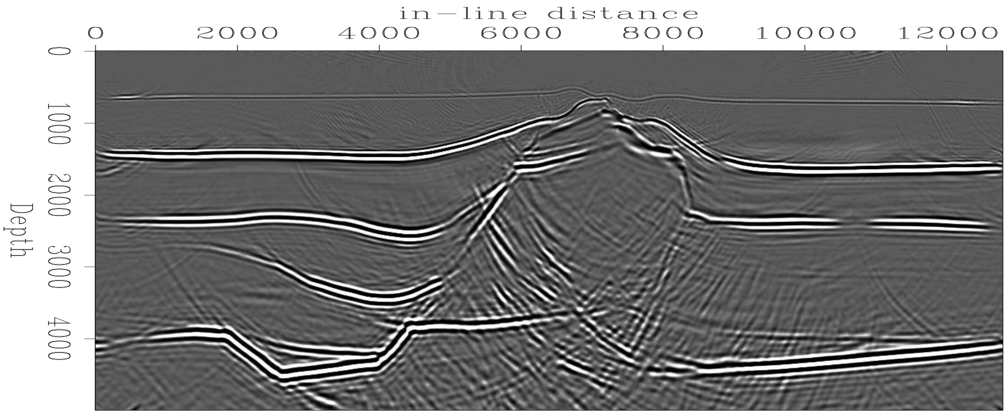

Figure 7: Extended split-step prestack migration with evanescent energy using 8 reference velocities. hermes1-ELFEVANESPRE [CR]

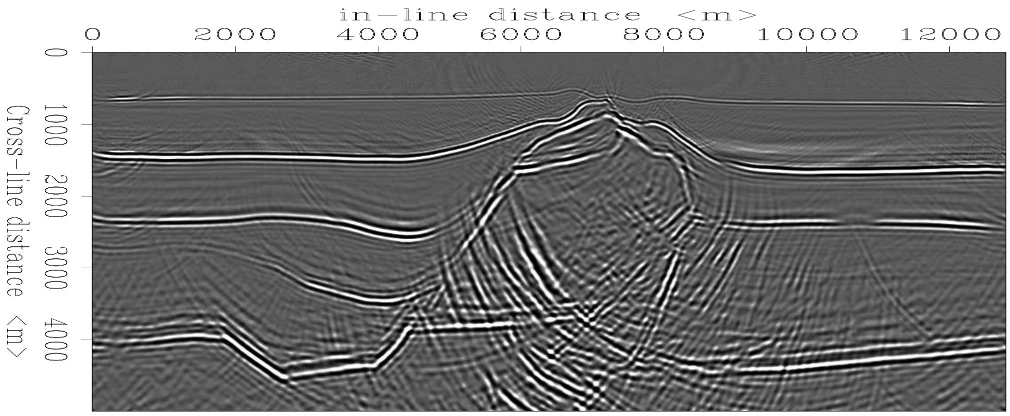

Figure 8: Extended split-step prestack migration with evanescent energy using 5 reference velocities and maximum offset 800m. Notice that the salt dome base is imaged reducing the number of offsets. hermes1-ELFEVANESPRE32full [CR]

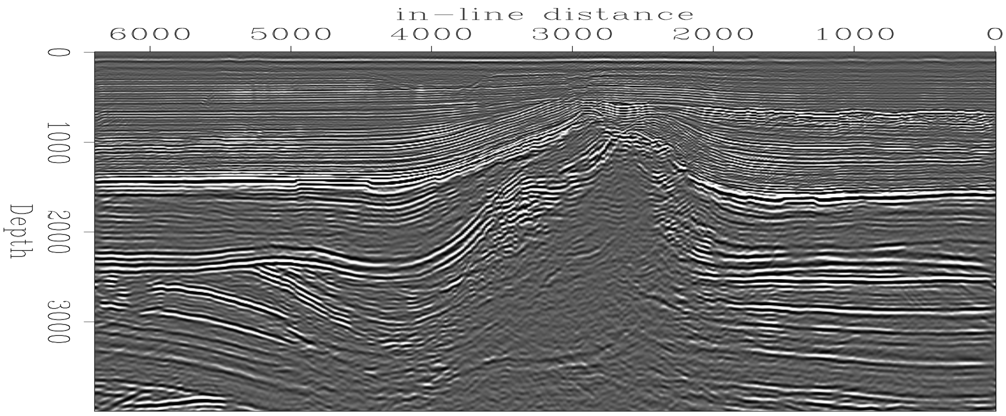

Figure 9: Extended split-step prestack migration of the real data set using 5 referenece velocities and with all the data offsets. hermes1-REALelf [CR]

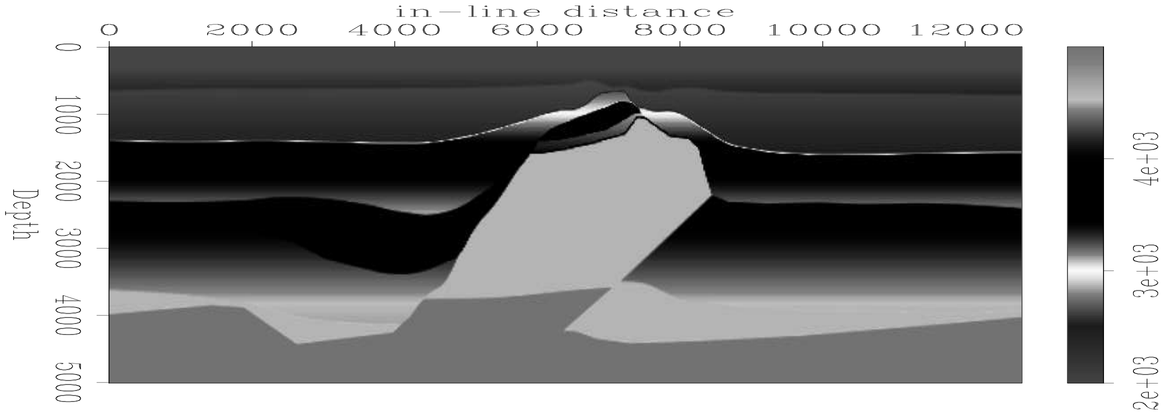

Figure 10: Salt dome velocity model (ELF-IFP). hermes1-ELFVEL [CR]

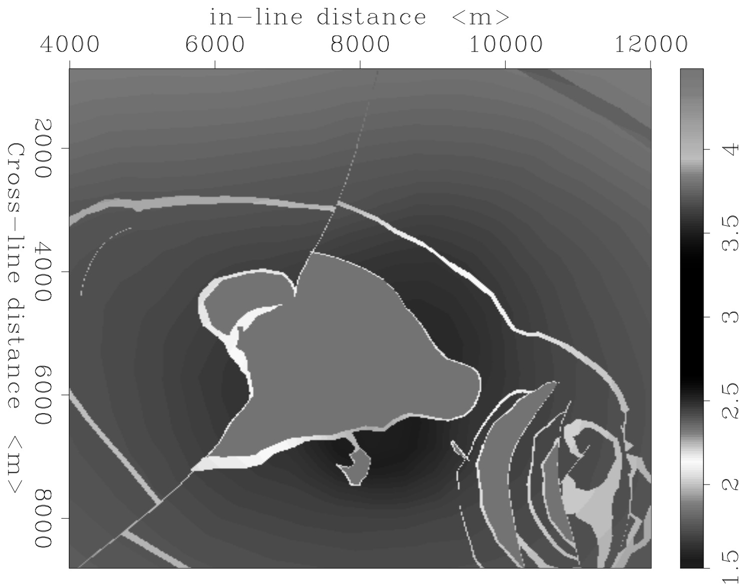

Figure 11: Velocity depth slice at 1300m of the SEG-EAEG model. hermes1-VelSEG1300 [CR]

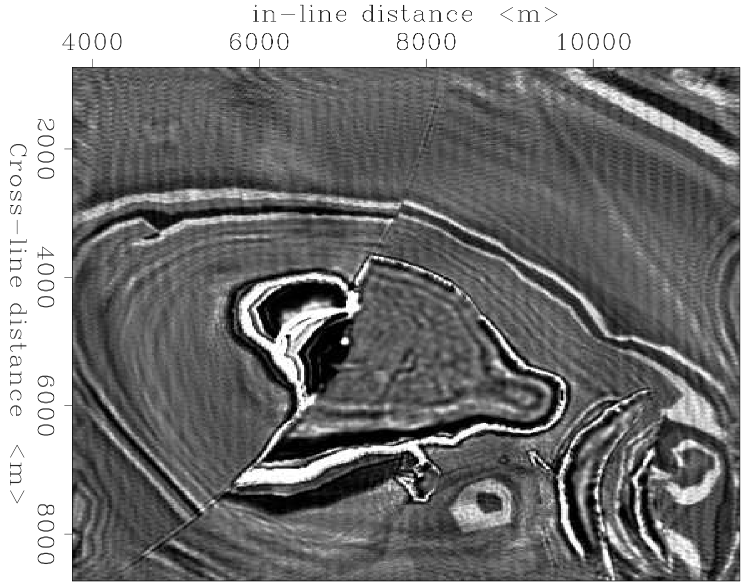

Figure 12: Depth slide at 1300m of the 3-D extended split-step zero-offset migration of the SEG-EAEG stack data using evanescent energy in the wavefield interpolation, and 10 reference velocities (see Figure 11). hermes1-SEGIN10v1300 [CR]

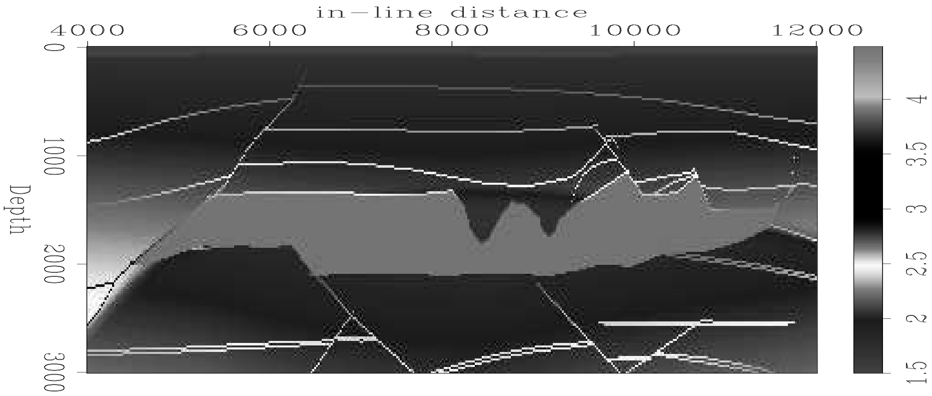

Figure 13: SEG-EAEG velocity field for the in-line section in Figure 14. hermes1-VelSEGVEL7500T [CR]

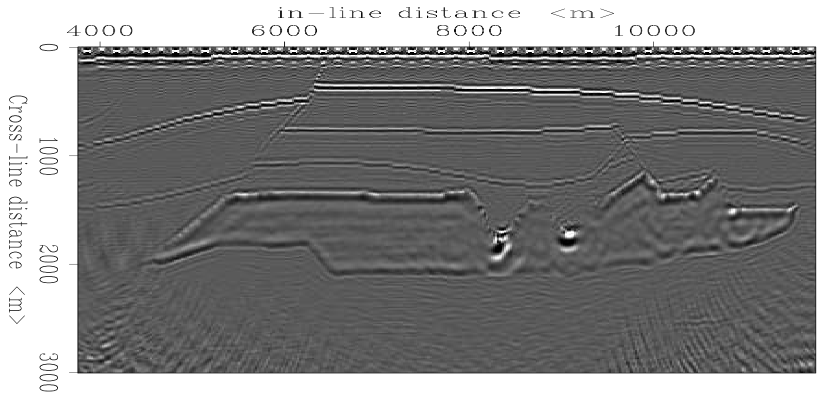

Figure 14: SEG-EAEG 3-D split-step migration using 10 reference velocities, in-line section at 7500m. hermes1-SEGIN10v7500T300 [CR]

REFERENCES

Biondi, B., and Palacharla, G., 1996, 3-D prestack depth migration of common-azimuth data: Geophysics, **61**, 1822–1832.

Gazdag, J., and Sguazzero, P., 1984, Migration of seismic data by phase shift plus interpolation: Geophysics, **49**, 124–131.

Herbert, V., 1992, Extended split-step Fourier migration: 62nd Ann. Int. Mtg., Soc. Expl. Geophys., Expanded Abstracts, 935–938.

Huang, L.-J., and Fechler, M. C., 1997, Extended pseudo-screen migration with multiple reference velocities: 67th Ann. Int. Mtg., Soc. Expl. Geophys., Expanded Abstracts, 1742–1745.

Kessinger, W., 1992, Extended split-step Fourier migration: 62nd Ann. Int. Mtg., Soc. Expl. Geophys., Expanded Abstracts, 917–920.

Stoffa, P. L., Fokkema, J. T., de Luna, R. M., and Kessinger, W. P., 1990, Split-step Fourier migration: Geophysics, **55**, 410–421.